Supporting Information

Trans-Cyclooctene-Functionalized PeptoBrushes with Improved Reaction Kinetics of the Tetrazine Ligation for Pretargeted Nuclear Imaging

E. Johanna L. Stéen[†¥‡], Jesper T. Jørgensen [¥‡], Kerstin Johann[§], Kamilla Nørregaard [¥‡], Barbara Sohr[¶], Dennis Svatunek[¶], Alexander Birke[§], Vladimir Shalgunov[†‡], Patricia E. Edem[†¥‡], Raffaella Rossin[‖], Christine Seidl[§], Friederike Schmid[#], Marc S. Robillard[‖], Jesper L. Kristensen[†], Hannes Mikula[¶], Matthias Barz[§], Andreas Kjær[¥‡*] and Matthias M. Herth[†¥*]*

[†]Department of Drug Design and Pharmacology, Faculty of Health and Medical Sciences, University of Copenhagen, Universitetsparken 2, 2100 Copenhagen, Denmark.

[¥]Department of Clinical Physiology, Nuclear Medicine & PET, Rigshospitalet, Blegdamsvej 9, 2100 Copenhagen, Denmark

[‡]Cluster for Molecular Imaging, Department of Biomedical Sciences, University of Copenhagen, Blegdamsvej 3, 2100 Copenhagen Ø, Denmark

[§]Institute of Organic Chemistry, Johannes Gutenberg University, Duesbergweg 10-14, D-55099 Mainz, Germany.

[¶] Institute of Applied Synthetic Chemistry, Technische Universität Wien (TU Wien), Getreidemarkt 9, 1060 Vienna, Austria.

[‖]Tagworks Pharmaceuticals, Geert Grooteplein 10, 6525 GA Nijmegen, Netherlands.

[#] Institute of Physics, Johannes Gutenberg University, Staudingerweg 7-9, D-55099 Mainz, Germany

Table of Contents

1. Theoretical analysis of reaction rate constants for the tetrazine ligation

We first consider the so-called Smoluchowski diffusion limit,[2] where one assumes that reactions take place instantaneously once the reaction partners meet. In that case, the effective reaction rate is determined by the rate with which such encounters take place. In free solution, the second order rate constant is given by the equation

$$k_0 = 4\pi R_0 D_0, \qquad \text{(Eq. 1)}$$

Where D_0 is the relative diffusion constant *i.e.*, the sum of the diffusion constants of the two reactants and R_0 the "capture radius", which is an effective parameter in the theory. The diffusion constants of the Tz-derivatives, D_H, and the TCO **16**, $D_{TCO\text{-}PEG}$, have been determined by fluorescence correlation spectroscopy (FCS) and DOSY NMR measurements. The result is D_H = 5.3 x 10^{-10} m^2/s for Tz **14**, D_H = 8.8 x 10^{-10} m^2/s for Tz **15**, and $D_{TCO\text{-}PEG}$ = 3.3 x 10^{-10} m^2/s for TCO-PEG **16** with a relative error of roughly 20%. Inserting the reaction rate k_{free} ~ 500/Ms (see table S1, for the reaction of **16** with Tz **15**) in Eq. (1), one would obtain the capture radius R_0 = 0.8 x 10^{-16} m for Tz **14** and R_0 = 0.5 x 10^{-16} m for Tz **15**, which is unphysically small. On the other hand, if one inserts a realistic value for R_0 of the order of 0.1–1 nm, one obtains a limiting Smoluchowski diffusion rate of the order of k_{free} ~ 10^9/Ms, which is much larger than the experimental value. Hence the reaction rate is controlled by a finite reaction probability rather than by diffusion.

Eq. (1) can be generalized for the case of finite bare reaction rates $k_{bare} < \infty$ following Collins and Kimball,[3] and one obtains

$$\frac{1}{k_{free}} = \left[\frac{1}{k_{bare}} + \frac{1}{4\pi R_0 D_0}\right]. \qquad \text{(Eq. 2)}$$

In our case, k_{bare} dominates, and we have $k = k_{bare}$ in free solution. This describes the reaction of **16** with the Tz-derivatives.

Next, we consider the situation when the TCO units are confined in the hydrophobic pockets of the PeptoBrushes. Since the Tz-derivatives are attracted to these pockets, they experience an attractive potential $U(R_0) < 0$. In general, applying the Smoluchowski theory to a situation with a distance dependent potential $U(r)$ and relative diffusion constant $D(r)$, we get the equation[4]

$$k_{brush} = 1 \Big/ \left[\frac{e^{\beta U(R_0)}}{k_{bare}} + \int_{R_0}^{\infty} dr \, \frac{e^{\beta U(r)}}{4\pi r^2 D(r)} \right], \qquad \text{(Eq. 3)}$$

with the Boltzmann factor $\beta = \frac{1}{k_B T}$. In the reaction rate-controlled limit of small k_{bare}, one obtains a solution to Eq. 3 that follows an Arrhenius law

$$k_{brush} = k_{bare} \, e^{-\beta U(R_0)} \qquad \text{(Eq. 4)}$$

Thus, the reaction rate increases in the brush. If we assume that the lipophilic Tz gain about 0.7 kcal/mol when associating with the hydrophobic pocket, a typical number for a hydrophobic interaction energy between nonpolar groups,[5] we obtain $\beta U(R_0) \sim -1.2$ and thus an increase in the reaction rate by roughly a factor $\frac{k_{brush}}{k_{bare}} \sim 3$. This is compatible with the increase of reaction rate between free TCO units in solution and TCO units on PeptoBrush **2** and **3**.

On the other hand, to obtain much larger values of k_{brush}/k_{bare}, one would have to significantly increase U. For example, an increase of a factor 29 could be obtained with a free energy of $\beta U(R_0) \sim 3.4$ or 2 kcal/mol, which would result in rather tightly bound Tz-derivatives. Hence, we would have to assume that increasing the TCO density in the brush from PeptoBrush **2** and **3** to PeptoBrush **1** leads to significant rearrangements of the polymer chains, such that several TCO

units cooperate to create pockets with a very high affinity to Tz-derivatives. This hypothesis is supported by the results of the simulations described in the main text.

In the computer simulations, the following potentials are used: All monomers interact *via* a repulsive Lennard-Jones potential of the form

$$U_{LJ}(r) = 4\,\varepsilon\left(\left(\frac{\sigma}{r}\right)^{12} - \left(\frac{\sigma}{r}\right)^{6} + \frac{1}{4}\right) \qquad \text{for } r < r_c \qquad \text{(Eq. 5)}$$

($U_{LJ}(r) = 0$ otherwise) with $r_c = \sqrt[6]{2}$. Monomer bonds are described by a FENE (Finite Extensible Nonlinear Elastic) potential of the form

$$U_{FENE} = -\frac{1}{2}\,k_b\,r_b^2\,\ln\left(1-\left(\frac{r}{r_b}\right)^2\right) \qquad \text{(Eq. 6)}$$

with $k_b = 30\frac{\varepsilon}{\sigma^2}$ and $r_b = 1.5\,\sigma$. In addition, monomers associated with TCO units interact with the following attractive potential:

$$U_{attr} = -\epsilon_a \frac{1}{1+\cos\left(\pi\left(\frac{r_c}{r_a}\right)^2\right)}\left(1+\cos\left(\pi\left(\frac{r}{r_a}\right)^2\right)\right) \qquad \text{(Eq. 7)}$$

with $r_a = 2\,\sigma$ and $\epsilon_a = 1.6\,\varepsilon$. With this choice of parameters, the minimum (non-bonded) interaction energy between TCO units is roughly given by $\bar{\epsilon}_{min} = -\epsilon_a$. The total value of the attractive energy in the system defines the "average number of TCO/TCO contacts per TCO", which is given by $U_{attr}/(\bar{\epsilon}_{min}N_{TCO})$, where N_{TCO} is the number of TCO units on the chain.

The simulations are carried at constant temperature $k_BT = 1\,\varepsilon$ using a Langevin thermostat.

2. Synthesis of monomers 5 and 13 for polymerization

*γ-Benzyl-L-glutamic acid N-carboxyanhydride (**5**).*

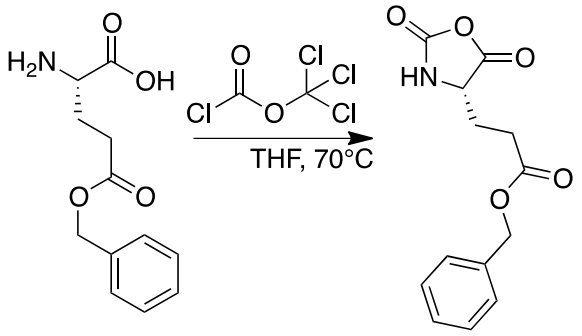

The synthesis of **5** was carried out as previously reported.[1] L-Glutamic acid 5-benzyl ester (10.1 g, 42.7 mmol) was thoroughly pestled and dried *in vacuo* in a flame-dried, 500 mL three-necked round bottom flask for 2 h. The flask was subsequently equipped with a stir bar, septum and reflux condenser connected to two gas washing flasks filled with NaOH (5.10 g, 0.13 mol) in water (250 mL). Freshly dried THF (200 mL) was added under nitrogen counter-flow suspending the amino acid. After ensuring a gas-tight apparatus by checking nitrogen leaving through the gas washing bottles, the nitrogen stream was stopped and diphosgene (4.1 mL, 34 mmol) was added slowly by syringe. The suspension was heated to 70 °C under stirring, yielding a clear and slightly yellow solution after 2 h. Then, the septum was exchanged with a quick-fit, fitted with a glass tube, through which a constant stream of nitrogen was bubbled through the solution for 3 h, removing excess phosgene, hydrogen chloride and THF. The reaction mixture was stored at -80 °C overnight. Remaining THF was removed *in vacuo* until a slightly yellow solid was obtained. The crude product was re-dissolved in THF (100 mL) and recrystallized from THF/hexane (1:1) twice. Crystallization was completed at -18 °C overnight and the product was filtered under dry nitrogen atmosphere, washed with hexane and dried first under a stream of nitrogen and finally under high vacuum to afford **5** (8.6 g, 76%) as colorless crystals. ^{1}H NMR (400 MHz, DMSO-d_6) δ 9.10

(s, 1H, CO-**NH**-CHR), 7.39–7.33 (m, 5H, **C**H_2-C_6**H**$_5$), 5.10 (s, 2H, **CH**$_2$-C_6H_5), 4.47 (ddd, *J* = 8.0 Hz, 5.6 Hz, 1.2 Hz, 1H, NH-**CH**-CO), 2.52 (m, 2H, CH_2-**CH**$_2$-CO), 2.10–1.88 (m, 2H, **CH**$_2$-CH_2-CO). Melting point: 93.6 °C (1 °C/min, starting at 85 °C).

*Sarcosine N-carboxyanhydride (**13**).*

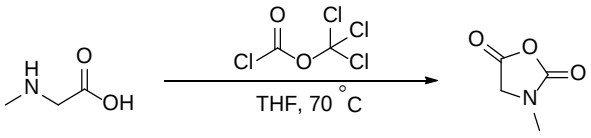

13

The synthesis of **13** was performed as described above for compound **5**.[1] Sarcosine (14.6 g, 0.16 mol) was dried *in vacuo* in a flame-dried, 500 mL three-necked round bottom flask for 2 h. The flask was subsequently equipped with a stir bar, septum and reflux condenser connected to two gas washing flasks filled with NaOH (19.7 g, 0.49 mol) in water (250 mL). Freshly dried THF (300 mL) was added under nitrogen counter-flow suspending the sarcosine. After ensuring a gas-tight apparatus by checking nitrogen leaving through the gas washing bottles, the nitrogen stream was turned off. Diphosgene (15.9 mL, 0.13 mol) was slowly added by syringe. The colorless suspension was heated to 70 °C under stirring, yielding a clear solution after 3 h. Thereafter, the septum was exchanged with a quick-fit, fitted with a glass tube, through which a constant stream of nitrogen was bubbled through the solution for 3 h, removing excess phosgene, hydrogen chloride and THF. The reaction mixture was stored at -80 °C overnight. Remaining THF was removed *in vacuo* until a brown solid was obtained. This solid was re-suspended in THF (60 mL) and precipitated into dry hexane (300 mL). The solution was cooled to -18 °C to complete precipitation and filtered under nitrogen atmosphere. The precipitate was washed with hexane and dried in a constant stream of nitrogen. The next day, the product was dried under high vacuum in a sublimation apparatus for 2 h and subsequently sublimated at 1×10^{-3} bar at 80 °C to afford **13** (11.4 g, 60%) as colorless crystals.

^{1}H NMR (400 MHz, DMSO-d_6) δ 4.22 (2 H, s, **CH$_2$**-CO), 2.86 (3H, s, N-**CH$_3$**). Melting point: 103.3 °C (1 °C/min, starting at 95 °C).

3. Synthesis of PeptoBrush 4

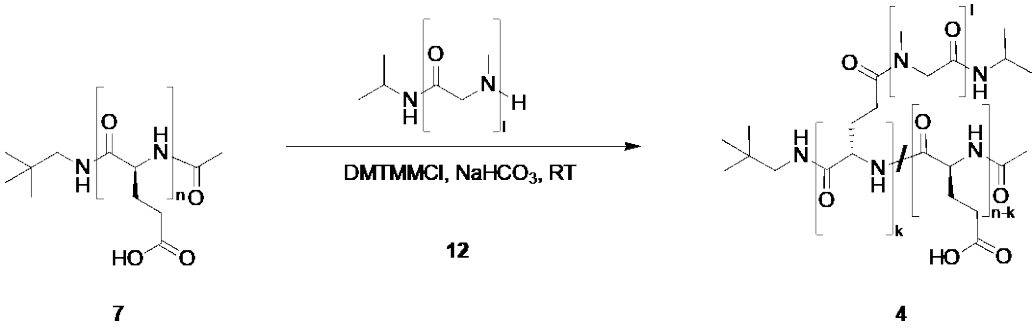

The synthesis where carried out as described for PeptoBrush **1**–**3** but without additional functionalization with **8.**

4. SEC characterizations for PeptoBrush 2, 3 and 4

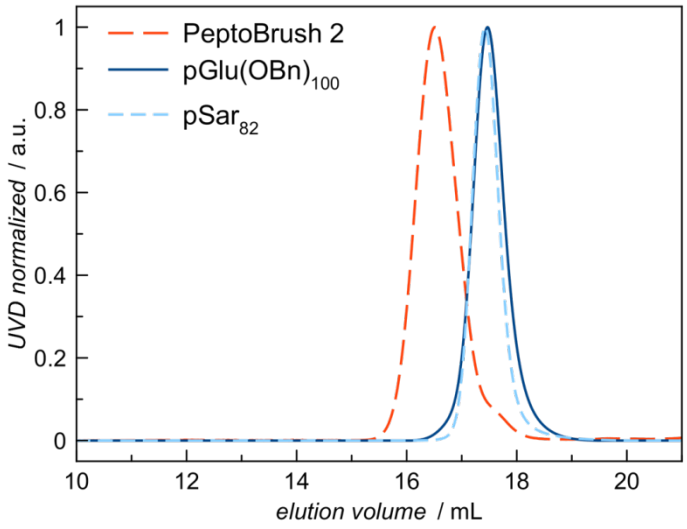

Figure S1. SEC characterization of pGlu(OBn)$_{100}$ (**6**), pSar$_{82}$ (**12**) and PeptoBrush **2**.

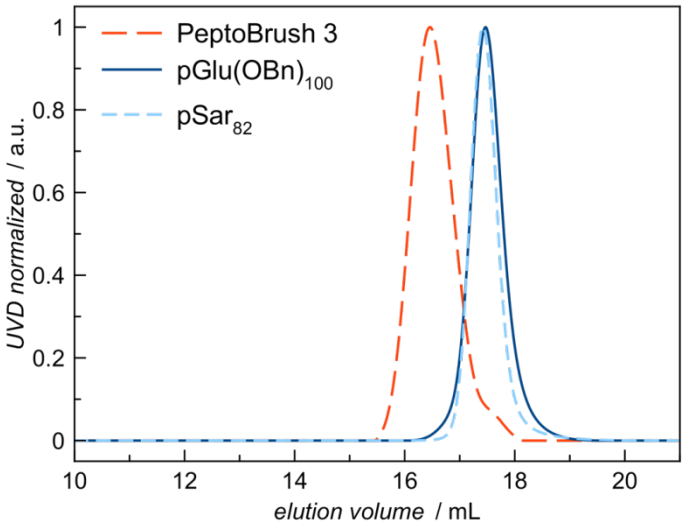

Figure S2. SEC characterization of pGlu(OBn)$_{100}$ (**6**), pSar$_{82}$ (**12**) and PeptoBrush **3**.

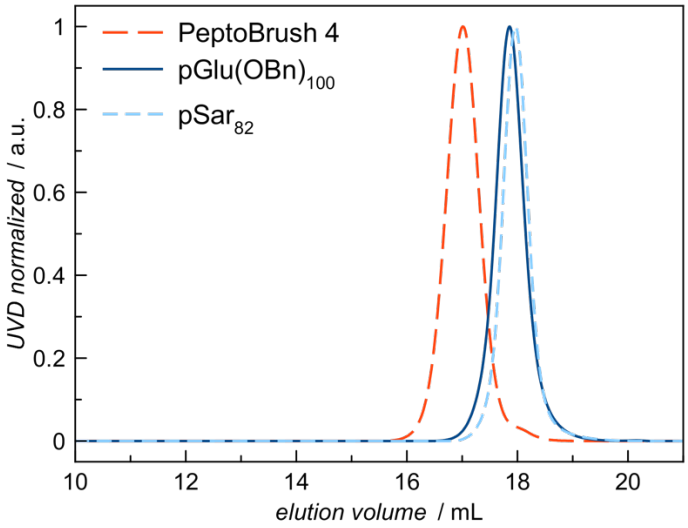

Figure S3. SEC characterization of pGlu(OBn)$_{100}$ (**6**), pSar$_{82}$ (**12**) and PeptoBrush **4**.

5. Dynamic light scattering plots for PeptoBrush 2, 3 and 4

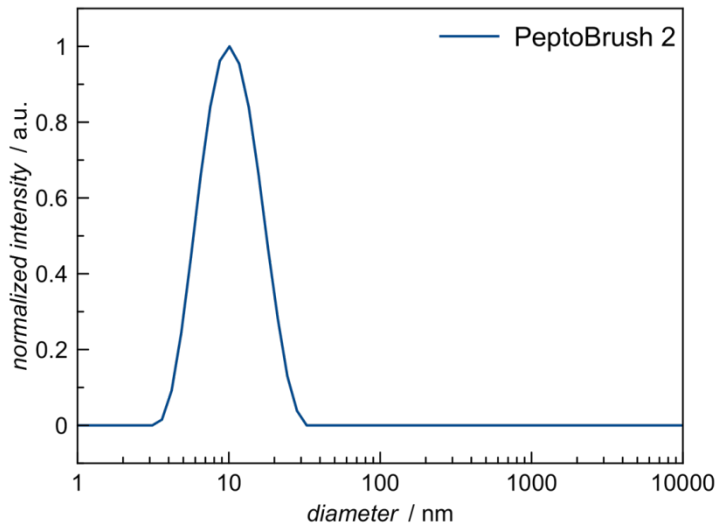

Figure S4. Dynamic light scattering (173°) of purified PeptoBrush 2.

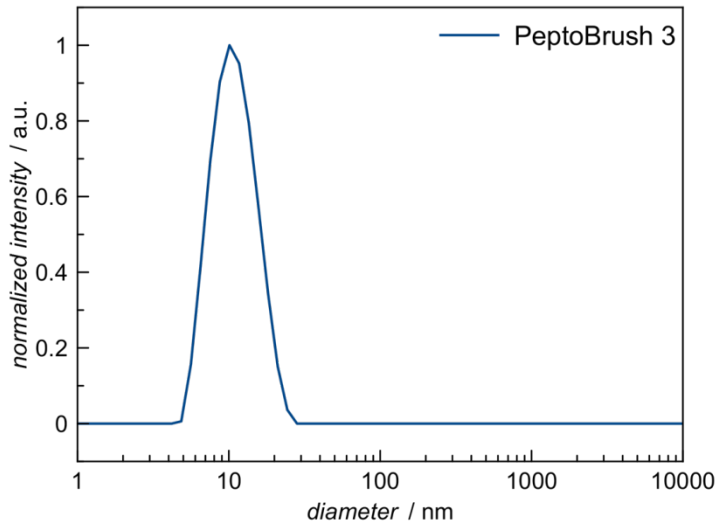

Figure S5. Dynamic light scattering (173°) of purified PeptoBrush **3**.

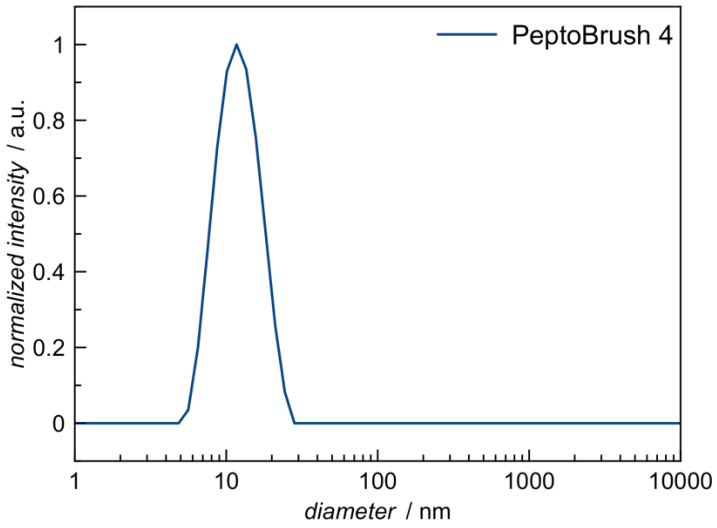

Figure S6. Dynamic light scattering (173°) of purified PeptoBrush **4**.

6. Kinetic measurements

Table S1: Reaction kinetics by stopped-flow spectrometry.

	TCO-loading[a]	Second order rate constant (M^{-1} s^{-1})[c]				Second order rate constant per TCO moiety (M^{-1} s^{-1})[c]			
		Tz **14**	Tz **15**	Tz **18**	Tz **19**	Tz **14**	Tz **15**	Tz **18**	Tz **19**
PeptoBrush **1**	30	336400	751400 118796[d]	159400	89874	11213	25047 3960[d]	5313	2996
PeptoBrush **1** (corrected)[b]	17.6	336400	751400 118796[d]	159400	89874	19114	42693 6750[d]	9057	5106
PeptoBrush **2**	13	24478	49712	-	-	1883	3824	-	-
PeptoBrush **3**	8	13253	15693	-	-	1657	1962	-	-
TCO derivative **16**	1	620	554 403[d]	7513	7455	620	554 403[d]	7513	7455

Notes: [a]TCO moieties per polymer determined by ^{1}H NMR in D_2O or DMSO-d_6. [b]Corrected TCO-loading based on reactive TCO moieties per polymer as determined by reaction with each Tz and UV/VIS spectroscopy. [c]Reaction rate measured in PBS at 37 °C (n = 5, standard deviation < 0.5%). [d]Reaction rate measured in full cell growth media (DMEM + 10% FBS) at 37 °C (n = 5, standard deviation < 0.5%).

Table S2. Concentrations used in kinetic investigations and observed and calculated rate constants.

TCO compound	Tz	$C_{polymer}$ (µM)	TCO-loading	C_{TCO} (µM)	k_{obs} (s^{-1})	k_2 ($M^{-1}s^{-1}$)	k_2 per TCO moiety ($M^{-1}s^{-1}$)
PeptoBrush 1	**14**	1.06	30	31.9	0.0634 ± 0.0009	119000 ± 57	3980 ± 2.0
	15				0.227 ± 0.003	427000 ± 180	14200 ± 6.0
PeptoBrush 2	**14**	1.78	13	26.7	0.0218 ± 0.0002	24500 ± 14	1880 ± 1.3
	15				0.0442 ± 0.0013	49700 ± 96	3820 ± 68.5
PeptoBrush 3	**14**	1.33	8	13.3	0.00884 ± 0.00012	13300 ± 17	1660 ± 2.7
	15				0.0105 ± 0.0001	15700 ± 17	1960 ± 2.6
16	**14**	50.7	1	50.7	0.0314 ± 0.00003	618 ± 0.5	618 ± 0.5
	15				0.0254 ± 0.0011	500 ± 23	500 ± 23

7. Determination of the number of reactive TCO moieties per polymer

Table S3. Concentrations and absorbance for the titration of PeptoBrush **1** with Tz **17**.

Total added equivalents of Tz	Total added µL of Tz solution	Total added mmol of Tz	Absorbance	V_{total} (µL)	c_{eff} (µM)
1.5	3.65	0.00036	0.14	1003.65	358.94
2	4.87	0.00048	0.21	1004.87	478.34
2.5	6.09	0.00060	0.29	1006.09	597.44
3	7.31	0.00072	0.36	1007.31	716.26
3.5	8.53	0.00084	0.44	1008.53	834.79

8. Stability of PeptoBrush 1 in human serum

To investigate the aggregation behavior of PeptoBrush **1** in human plasma, plasma pooled from 6 patients was used. The plasma was obtained from the University Medical Center of the Johannes Gutenberg University Mainz (Germany). The plasma was filtered through a Millex GS 0.22 µm filter (Millipore). PeptoBrush **1** and DPBS were filtered through 0.2 µm pore size Millex GHP filters (Millipore). The following mixtures have been prepared: plasma:DPBS 9:1 and plasma: PeptoBrush **1** 9:1 ($c_{PB4} = 3.4 \cdot 10^{-8}$ M). The cuvettes were incubated for 20 min at room temperature before measurement. Analysis was done according to Rausch *et al.*[6]

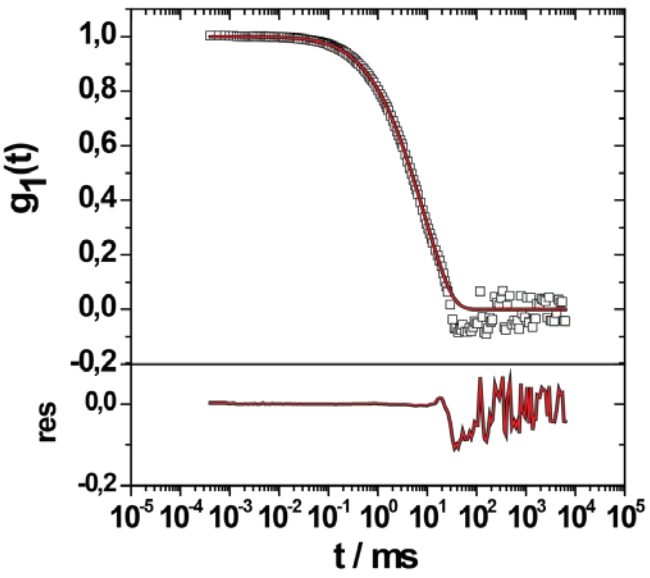

Figure S7. Multi-angle dynamic light scattering of purified PeptoBrush **1** in 90% human serum by DLS at 30°. □ Squares: Autocorrelation function $g_1(t)$ recorded from PeptoBrush **1** in 90% human serum. Red line: Force fit. Black line: Fit with a variable component.

9. Ligation reactivity of PeptoBrush 1 in mouse serum and phosphate buffered saline

The plasma half-live of TCO moieties in PeptoBrush **1** were investigated *in vitro* using mouse plasma and PBS. Results are presented in Figure S8. Apparent TCO half-lives obtained by fitting a mono-exponential decay function with a fixed initial value on the ligation reactivity data are 45 h for plasma and 198 h for PBS. Points represent mean values of 2–4 determinations from two independent experiments, error bars represent standard deviations.

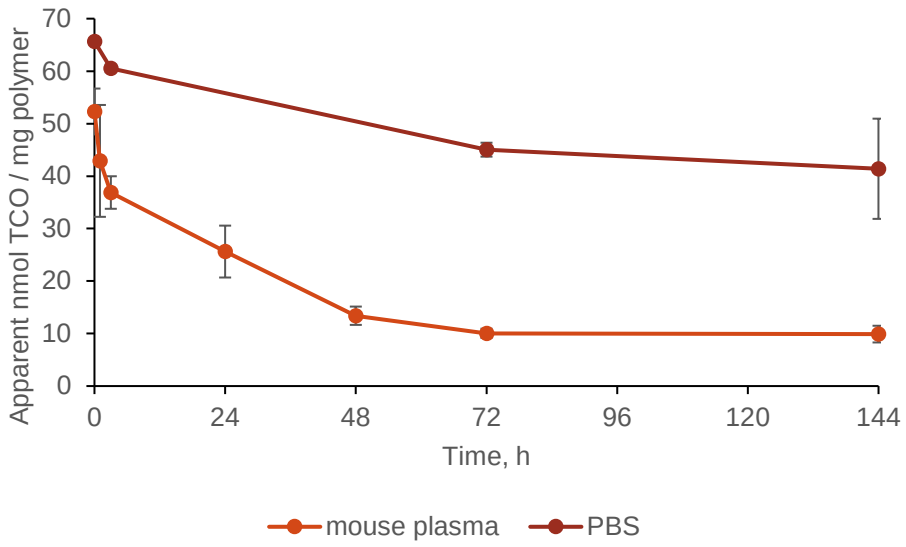

Figure S8. Changes in apparent ligation reactivity of TCO moieties in PeptoBrush 1 during incubation in PBS and mouse plasma.

Methods

Precast NuPAGE 4−12% Bis-Tris sodium dodecyl sulfate polyacrylamide gel electrophoresis (SDS-PAGE) gels, NuPAGE MES SDS running buffer (20X), NuPAGE LDS sample buffer (4X), and SeeBlue® Plus2 Pre-Stained Protein Standard were obtained from Invitrogen (USA).

100 μg/mL solutions of PeptoBrush **1** in PBS (10 mM phosphate buffer, 120 mM NaCl, pH 7.2) and Balb/c mouse plasma were prepared from 2 mg/mL stock of PeptoBrush **1** in PBS. Thus,

PeptoBrush **1** solution in plasma consisted of 95% plasma and 5% PBS (v/v). These solutions were incubated at 38 °C with shaking at 800 rpm for 144 h. Before the start of the incubation ("0 h" time point) and at 1 h, 3 h, 24 h, 48 h, 72 h and 144 h after the start of the incubation, 15 μL aliquots were withdrawn for TCO titration. From the PBS solution, aliquots were only withdrawn at 0, 3, 72 and 144 h. Each aliquot was mixed with 5 μL of ^{111}In-labeled Tz solution (45 μM [^{111}In]**20** in 0.1M NH_4OAc buffer pH 5 with 0.1 mg/mL gentisic acid). Resulting mixtures were left standing at room temperature for at least 1 h to ensure full consumption of reactive TCO moieties. Then, samples of 3–9 μL were taken from the mixtures, diluted 2–4 fold with water, mixed with NuPage LDS Sample buffer according to the instructions provided from the supplier, heated for 10 min at 70 °C and applied on the NuPAGE 4−12% Bis-Tris SDS-PAGE gels. SDS-PAGE was run in MES-SDS buffer at 150V for 40–45 min. Separation was monitored by running SeeBlue® Plus2 Pre-Stained Protein Standard along with radiolabeled polymer samples. Control mixtures of 5 μL of [^{111}In]**20** solution with 15 μL of plasma were prepared and processed in the same manner. Developed gels were exposed against phosphor storage screens (PerkinElmer Multisensitive), which were then read in the Cyclone Plus phosphorimager (Packard Instruments, USA). Autoradiograms were quantified using Optiquant 3.0 software (Packard Instruments). Radioactivity found in the section of the gel corresponding to molecular weights of 60 kDa and above (using SeeBlue standards as reference) was considered polymer-bound.

Apparent TCO-loading of the polymer (m_{TCO}, nmol/mg) was calculated according to the formula:

$$m_{TCO} = \%bound \times \frac{n_{Tz}}{m_{PB}}, \qquad \text{(Eq. 8)}$$

where *%bound* is the percentage of ^{111}In activity bound to the polymer, while n_{Tz}/m_{PB} is the ratio of the amount of Tz and the mass of PeptoBrush **1** used in the titration. In the described experiment, n_{Tz}/m_{PB} was fixed and equal to 0.225 nmol Tz per 1.5×10^{-3} mg PeptoBrush **1**, or 150 nmol/mg.

For both PBS and mouse plasma, two independent experiments were performed in parallel. For each time point, from one of the experiments, chosen in an alternating manner, two aliquots for TCO titration instead of one were withdrawn and analysed separately.

10. Radiochemistry

*^{111}In-labeling of DOTA-functionalized tetrazine **19***

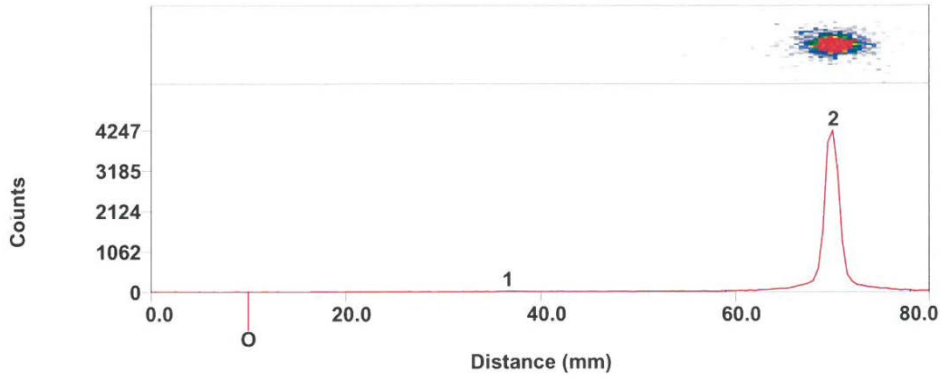

ID	Gross Counts	Baseline Subtract	Net Counts	Net CPM	Net % Sum Regions	Net % Total Lane
Lane #1						
1-1	469	0	469	760.54	2.4	2.3
1-2	18,733	0	18,733	30,377.84	97.6	93.7
Lane	20,001	0	20,001	32,434.05		100.0
Unres	799	0	799	1,295.68		4.0

Figure S9. Radio-TLC for ^{111}In-labeling of DOTA-Tz **19**. TLC-eluent: 200 mM ethylenediaminetetraacetic acid, (EDTA).

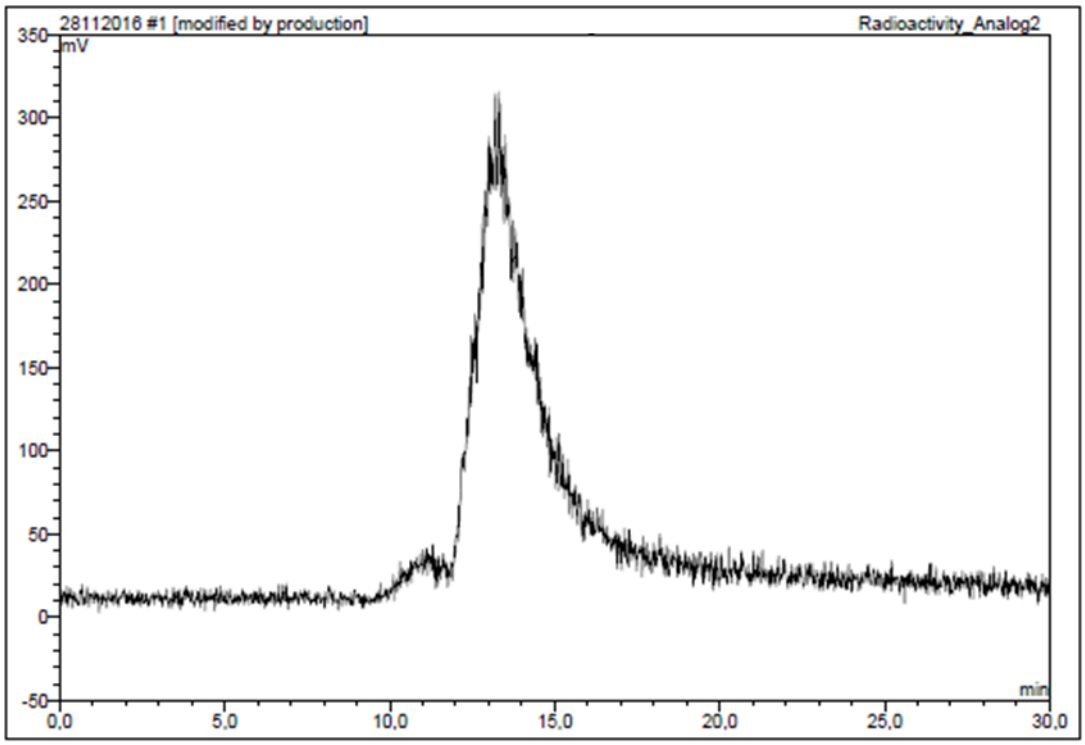

Figure S10. Radio-HPLC chromatogram for ^{111}In-labeled Tz ([^{111}In]**20**).

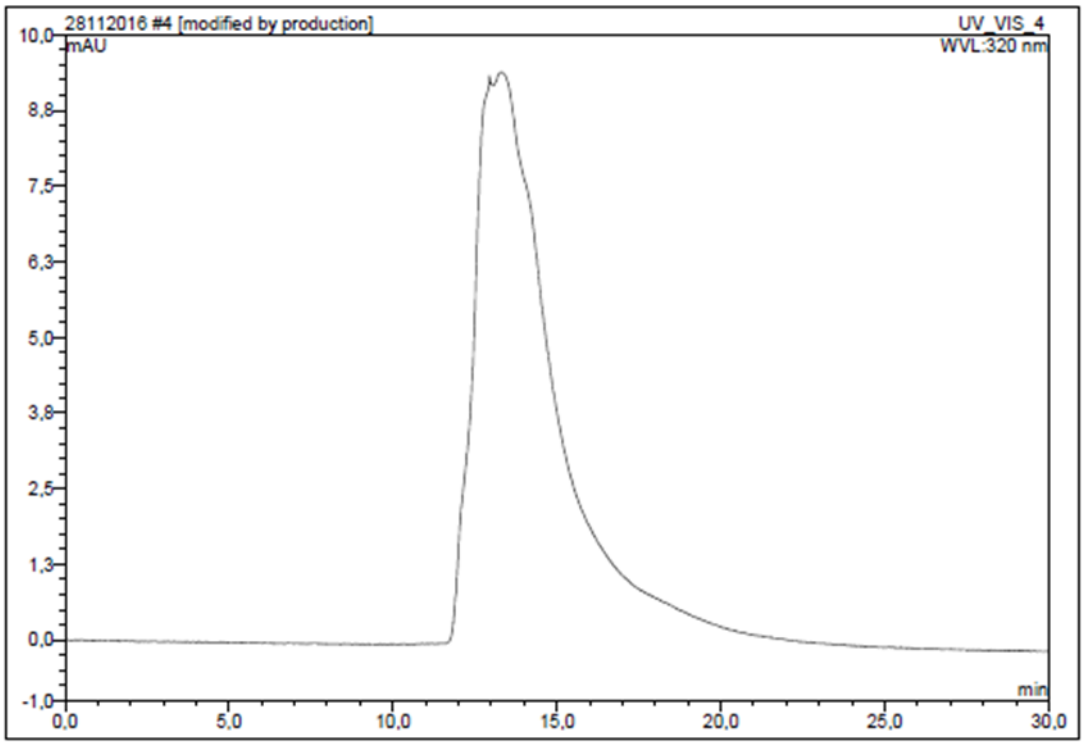

Figure S11. HPLC chromatogram for DOTA-Tz **19**.

*Ligation between PeptoBrush **1** and [^{111}In]**20***

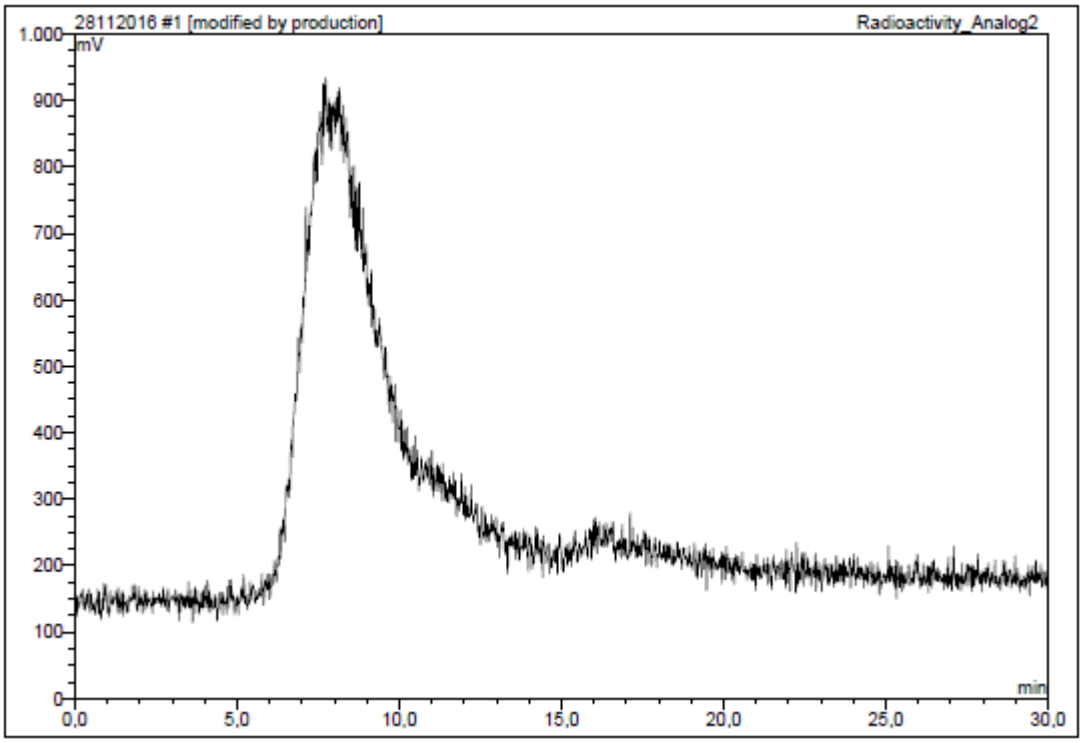

Figure S12. Radio-HPLC chromatogram for ^{111}In-labeled PeptoBrush **1** ([^{111}In]**21**).

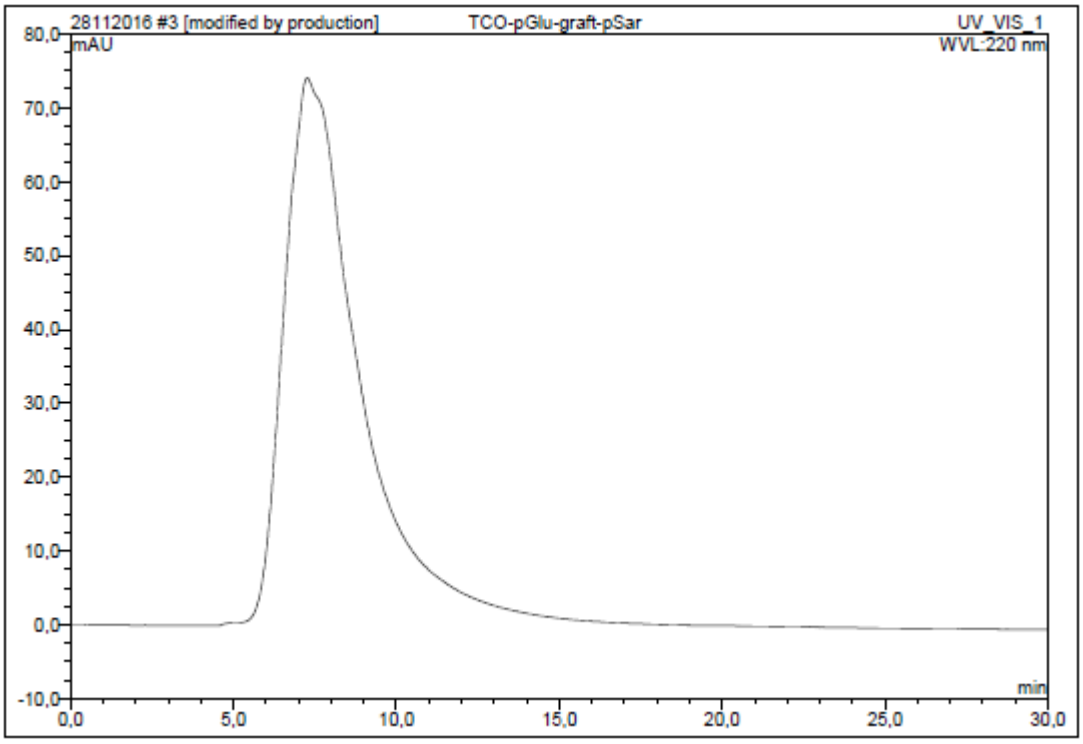

Figure S13. HPLC chromatogram for PeptoBrush **1**.

11. Determination of the biodistribution of [^{111}In]20 using SPECT/CT imaging

SPECT/CT imaging was carried out as described in the experimental section of the manuscript. Four animals received [^{111}In]**20** (~50 MBq, 95 µL, apparent A_m = 5.4 GBq/µmol). As early as 2 h after injection, all quantified tissues had a mean uptake below 0.3 %ID/g, except for the kidneys, which [^{111}In]**20** is excreted through.

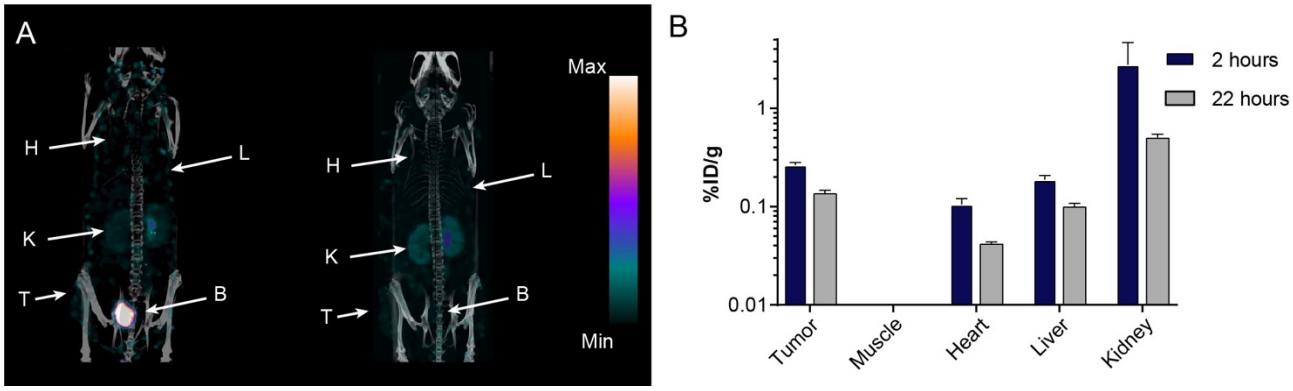

Figure S14. (A) Representative SPECT/CT images (maximum intensity projection) of animals that only received [^{111}In]**20**, followed by SPECT/CT imaging at 2 h and 22 h p.i. Abbreviations: H = heart, L = liver, K = Kidney, B = bladder, and T = tumor. (B) Mean uptake in tissues from animals that only received [^{111}In]**20**. Uptake in muscle tissue was too low to be detected. Data represented on a log scale to show very low uptake values. *n* = 4 for each group. Data represent mean ± S.E.M.

12. Optimization of timing – 500 µg dose of [^{111}In]21

Experiments were carried out as described in the materials and methods section of the manuscript. Briefly, CT26 tumor-bearing animals (*n* = 3 mice per time point) were administered with 500 µg of [^{111}In]**21** (~8 MBq, 100 µL, apparent A_s = 13 MBq/mg). At 2 h, 22 h, 48 h, 72 h, 96 h, 120 h, and 144 h p.i. The mice were euthanized, tissue resected, weighed and the radioactivity fraction in each tissue was measured in a gamma counter.

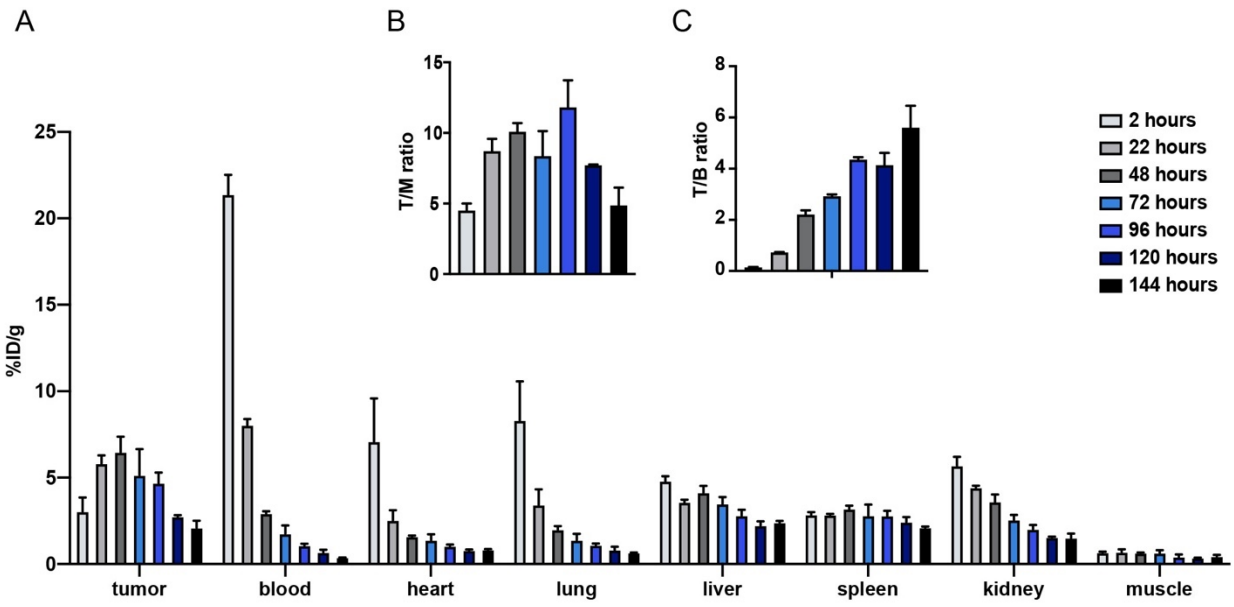

Figure S15. (A) *Ex vivo* biodistribution showing uptake values (%ID/g), (B) Tumor-to-muscle (T/M) ratios and (C) Tumor-to-blood (T/B) ratios at different time points for CT26 tumor-bearing mice injected with 500 µg of [^{111}In]**21 (***n* = 3 for each time point). Data are shown as mean and standard error of mean (S.E.M.).

13. Conventional SPECT/CT imaging with 100 µg dose of [^{111}In]20

SPECT/CT imaging was carried out as described in the experimental section of the manuscript. Four animals received 100 µg of [^{111}In]**21**(~10 MBq, apparent A_s = 114 MBq/mg) and were SPECT/CT scanned 2 h, 22 h and 72 h 2 h after injection.

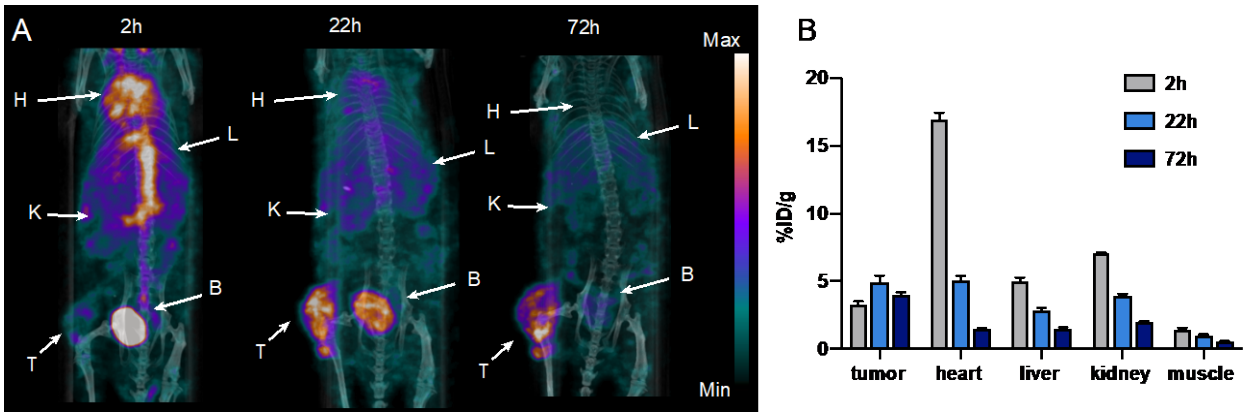

Figure S16. (A) Representative SPECT/CT images (maximum intensity projection) at 2 h, 22 h and 72 h after injection of 100 µg of [^{111}In]**21** in CT26 tumor-bearing mice. Each image is scaled between its minimum and maximum pixel intensity. (B) Image derived mean uptake values (%ID/g) in tissues (*n* = 4).

14. Biodistribution studies

Table S4. Mean T/M and mean T/B ratios determined by conventional imaging of PeptoBrush **1** using a dose of 1 mg.

T/M			**T/B**		
2 h	**22 h**	**72 h**	**2 h**	**22 h**	**72 h**
2.6	6.7	11.6	0.2	1.0	2.8

Table S5. *Ex vivo* biodistribution, pretargeting study using 50 μg, 100 μg, 250 μg and 500 μg, lag time 72 h, determined 2 h p.i. of [^{111}In]**20**.

PeptoBrush 1 (□g)	**%ID/g** ($p > 0.05$)
50	0.51 ± 0.05
100	0.51 ± 0.03
250	0.78 ± 0.03
500	1.45 ± 0.38

Table S6. Pretargeted imaging mean T/M and mean T/B ratios (100 μg) PeptoBrush **1** 72 h injected before [^{111}In]**20)**

T/M		**T/B**	
2 h	**22 h**	**2 h**	**22 h**
4.4	6.5	1	1.5

15. NMR spectra for polymer synthesis

*γ-Benzyl-L-glutamic acid N-carboxyanhydride (**5**)*

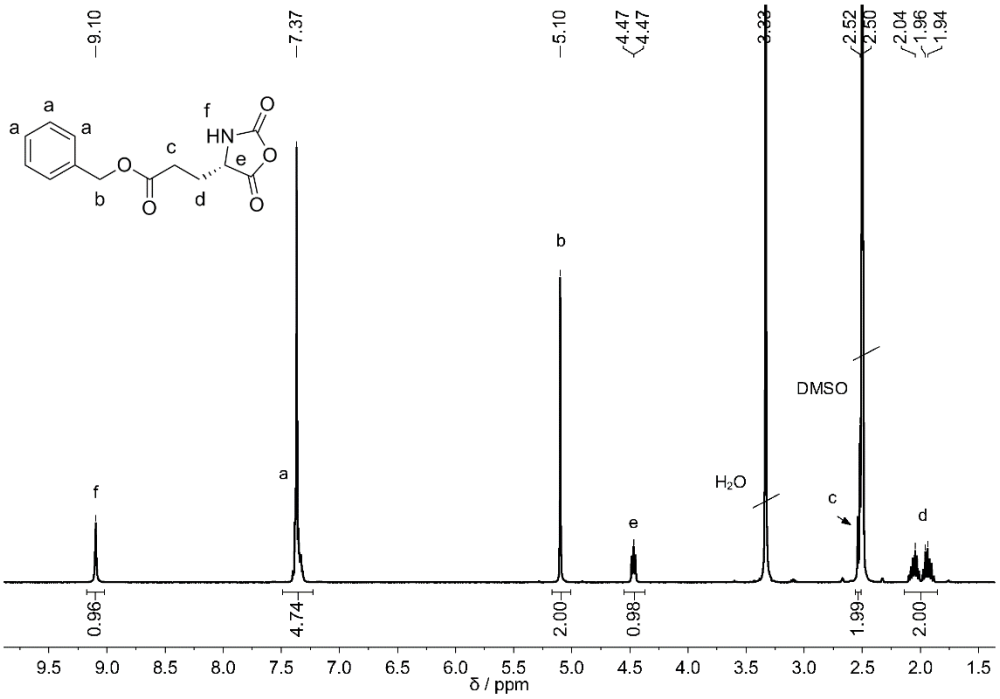

*Sarcosine N-carboxyanhydride (**13**)*

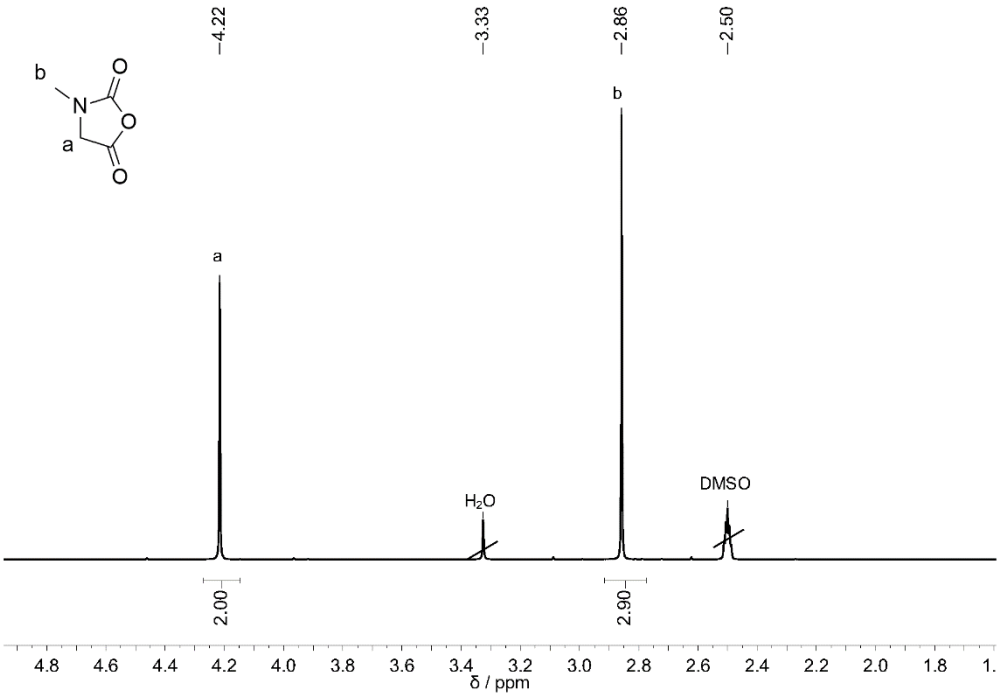

*Poly(γ-benzyl-L-glutamic acid) (**6**)*

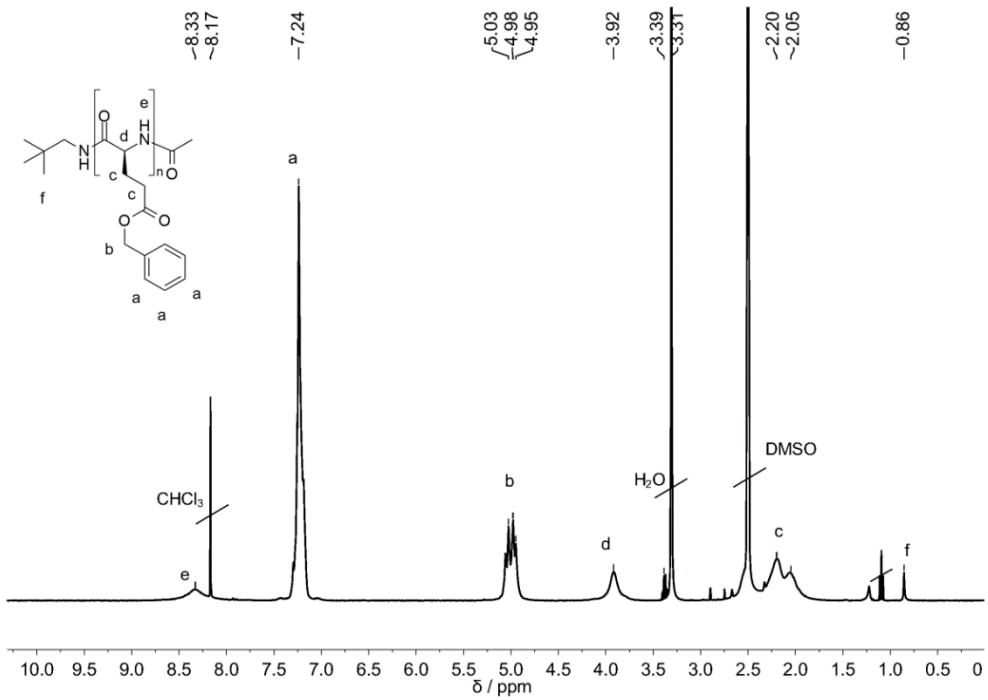

*Polyglutamic acid (**7**)*

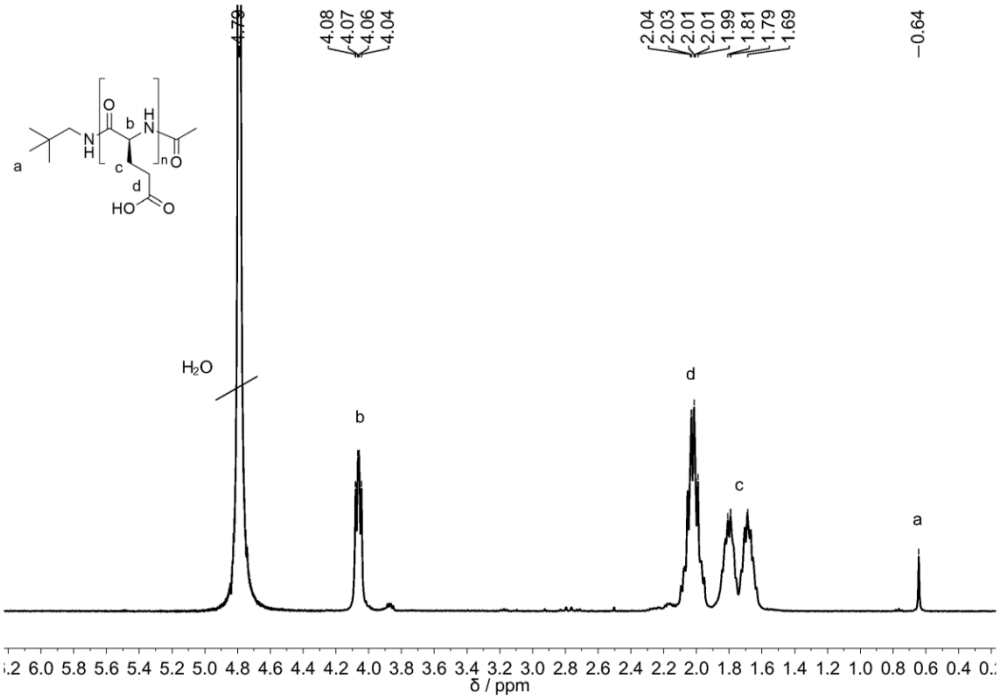

*Polysarcosine (**12**)*

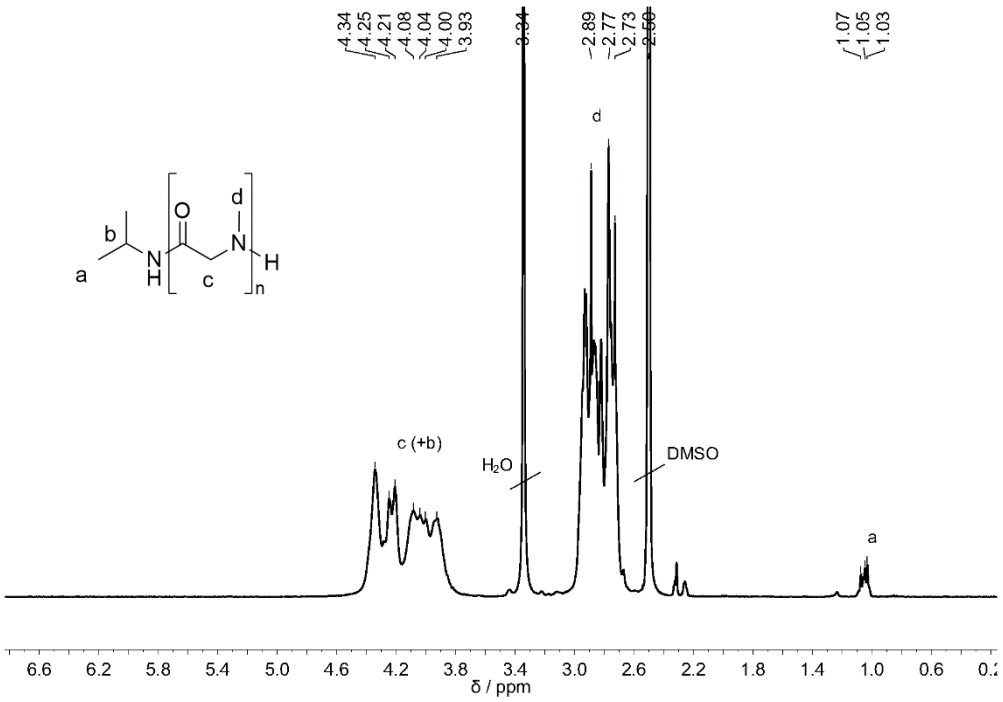

*PeptoBrushes **9**–**11***

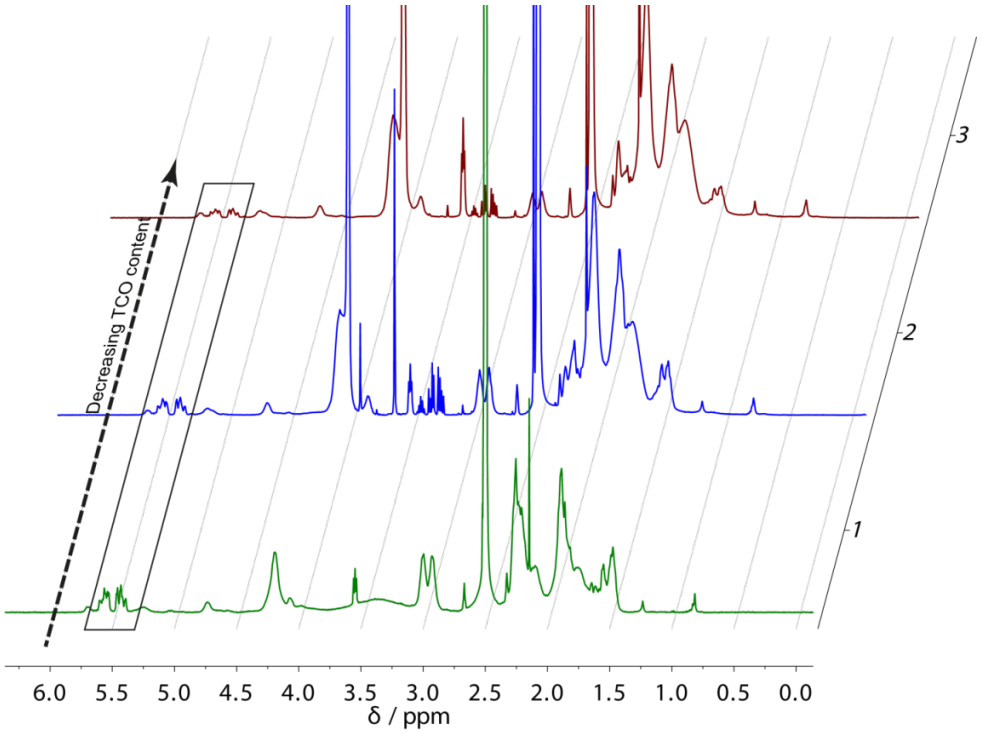

*PeptoBrush **1** stacked with **7** and **9***

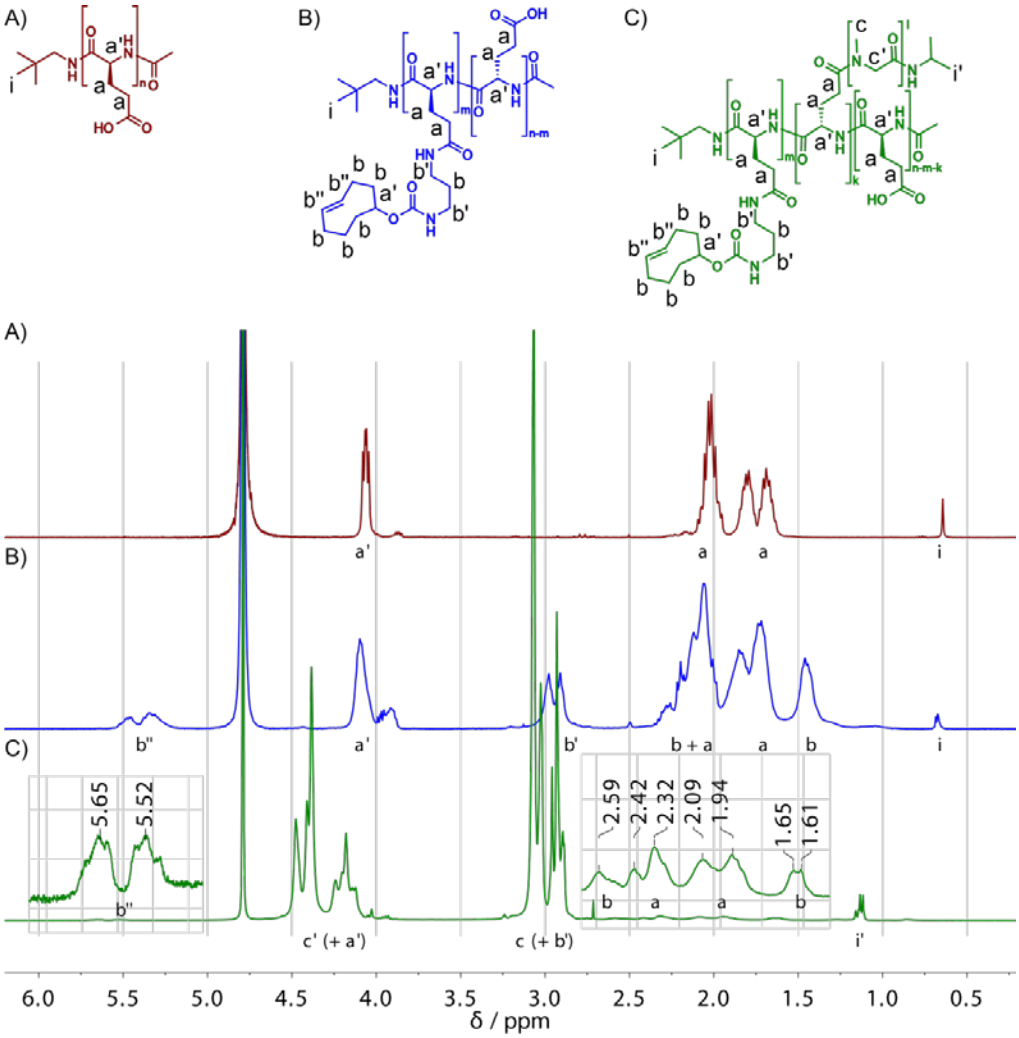

16. References

1. Birke, A.; Huesmann, D.; Kelsch, A.; Weilbacher, M.; Xie, J.; Bros, M.; Bopp, T.; Becker, C.; Landfester, K.; Barz, M. Polypeptoid-Block-Polypeptide Copolymers: Synthesis, Characterization, and Application of Amphiphilic Block Copolypept(o)ides in Drug Formulations and Miniemulsion Techniques. *Biomacromolecules*. **2014**, *15*, 548–557.
2. Smoluchowski, M. Versuch einer Mathematischen Theorie der Koagulationskinetik Kolloider Loesungen. *Z. Phys. Chem*. **1917**, *92*, 129–168.

3. Collins, F. C.; Kimball, G. E. Diffusion-Controlled Reaction Rates. *J. Colloid Sci.* **1949**, *4*, 425–437.
4. Schulten, K.; Kosztin, I. Lectures in Theoretical Biophysics, Univ. of Illinois, **2000**, https://www.ks.uiuc.edu/Services/Class/NSM.pdf (Accessed October 13th).
5. Andrews, P. R.; Craik, D. J.; Martin, J. L. Functional Group Contributions to Drug-Receptor Interactions. *J. Med. Chem.* **1984**, *27*, 1648–1657.
6. Rausch, K.; Reuter, A.; Fischer, K.; Schmidt, M. Evaluation of Nanoparticle Aggregation in Human Blood Serum. *Biomacromolecules.* **2010**, *11*, 2836–2839.